

Thiadiazole derivatives as inhibitors for acidic media corrosion of artificially patinated bronze

S. Varvara*, R. Bostan, L. Găină and L. M. Muresan*

Electrochemical impedance spectroscopy (EIS) and SEM-EDX observations were used to evaluate the inhibiting effect of four thiadiazole derivatives, i.e. 2-mercapto-5-amino-1,3,4-thiadiazole (MAT), 2-mercapto-5-methyl-1,3,4-thiadiazole (MMeT), 2-mercapto-5-acetylamino-1,3,4-thiadiazole (MAcAT) and 2-mercapto-5-phenylamino-1,3,4-thiadiazole (MPhAT) on the corrosion of naked and artificially patinated bronze surface exposed to an acidic solution (pH 3) that simulates a strongly polluted rainfall. For comparison reasons, the inhibiting effect of benzotriazole (BTA) was also examined. In an attempt to better understand the influence of solution pH on the adsorption of the thiadiazole derivatives and to correlate their structural and electronic characteristics with the experimental inhibition efficiencies, quantum chemical calculations were performed starting with thiadiazole and its protonated derivatives. Finally, a possible inhibition mechanism of the thiadiazole protonated species on bronze corrosion was proposed. It was concluded that MMeT and MAT allow the stabilization of the patina layer, leading to the protection of the bronze substrate and their effectiveness significantly increase with the immersion time.

1 Introduction

When exposed to atmospheric conditions, copper and its alloys form thin layers of corrosion products, called patina, having characteristic colours, from bluish and green to brown and even black and conferring antiquity and aesthetically pleasant aspects to the object [1–3]. On the other hand, the patina can be generated also artificially, for aesthetic reasons or for scientific research purposes. Once formed, the patina is relative stable and acts as a protective barrier of the bronze objects under many exposure conditions [4,5].

During the last century, the increasing of atmospheric pollution and especially the acid rain phenomenon induced a significant change in the nature and properties of copper-based

patina [1,6,7]. Thus, under the influence of the environment, the patina may become unstable and the corrosion processes could accelerate [5], leading not only to a discoloration of the original surface, but also to a serious degradation of the metallic surface [8].

In the last years, the consciousness towards the care of the cultural heritage has been stimulated and the protection of both historical monuments and modern artistic works encouraged. Various investigations have been conducted to understand the corrosion processes, the morphology and mechanism of patinas formation on copper and its alloys [1–3,9–16]. In order to reduce the degradation of metallic cultural heritage, suitable conservation treatments with protective substances that enable the preservation of the objects and the information they carry-on into the future [17] are often required. In this view, there is a continuous search in field of metal conservation for finding new improved corrosion inhibitors that provide a better protection to the cultural heritage objects, while respect both, the special requirements of the conservation-restoration ethics [18] and the ecological policies for the use of the chemicals [19]. It should be emphasized that, compared to industrial applications, where the anticorrosive effectiveness and the lack of toxicity of the corrosion inhibitors are the key parameters for their selection [18], in the case of cultural heritage conservation treatments, the use of these substances is restricted by several factors, such as the composition alterations, colour changes, toxicity and inhibitor film stability [20,21].

To this regard, a range of organic corrosion inhibitors, mainly nitrogen and sulphur-containing organic heterocyclic

S. Varvara, R. Bostan

Department of Exact Sciences and Engineering, “1 Decembrie 1918” University, 11–13 Nicolae Iorga St.510009, Alba Iulia (Romania)
E-mail: svarvara@uab.ro

R. Bostan, L. M. Muresan

Department of Chemical Engineering, “Babes-Bolyai” University, 11 Arany Janos St.400028, Cluj-Napoca (Romania)
E-mail: limur@chem.ubbcluj.ro

L. Găină

Department of Chemistry, “Babes-Bolyai” University, 11 Arany Janos St.400028, Cluj-Napoca (Romania)

compounds, developed for industry, were tested as corrosion inhibitors of copper and bronze historical objects [22]. Among them, benzotriazole (BTA) has been known since 1947 to be a very effective corrosion inhibitor for copper and its alloys [23] over a wide temperature and pH range, being considered as the most efficient inhibitor in the consolidation and conservation treatment of bronze artefacts. The effectiveness of BTA has been related to its adsorption on the metallic surface and formation of a $[\text{Cu}^+\text{BTA}]_n$ polymeric complex [24], which gives rise to a very thin, but effective protective film [25]. However, in strong acidic solutions, BTA exists predominantly as protonated species, BTAH^+ , which is less strongly chemisorbed on the electrodic surface, as the metal is thought to be positively charged in these solutions [26]. This leads to a decrease of the BTA inhibition efficiency in highly acidic solution. For instance, *Golfomitsou* and *Merkel* [27] have shown that BTA fails to inhibit the corrosion of heavily degraded artefacts where the pH level is low, such as in the case of pitting and active bronze disease. Moreover, BTA has proved to be much less efficient in the case of bronze than on copper [28], due to the scarce reactivity of BTA with the lead and tin in the alloy [29]. Additionally, recent studies [20,21] showed that the stabilization of bronze artefacts with BTA is not always successful; the treatment might alter the appearance of the patina layer, by darkening the mineralized surfaces containing cuprites, malachite and nantokite. Apart from these, the most serious deficiency of BTA is the fact that it is a harmful substance, which cannot be biodegraded [28,30].

The literature indicates that some triazoles [31] and imidazole derivatives [32–34] are effective in the reinforcement of artificial protective patinas on bronze in weak acidic solutions (pH 5), but their effectiveness is lower than that of BTA.

In a recent paper, some innocuous thiadiazole derivatives, i.e. 2-mercapto-5-amino-1,3,4-thiadiazole (MAT), 2-mercapto-5-acetyl-amino-1,3,4-thiadiazole (MAcAT), 2-mercapto-5-methyl-1,3,4-thiadiazole (MMeT) and 2-mercapto-5-phenylamino-1,3,4-thiadiazole (MPhAT), were reported as corrosion inhibitors of bronze in weakly acidic media (pH 5). The results showed that the protection effectiveness of the thiadiazole derivatives on bronze corrosion strongly depends on their molecular structure, particularly on the size and electronic effects of the substituents, as shown in the following sequence: MPhAT (97%) > MAT (95.9%) > MAcAT (95.7%) > MMeT (92.6%) [35]. Moreover, electrochemical tests carried out in weakly acidic artificial rain (pH 5) show that MAcAT and MAT at a concentration of 1 mM also efficiently hinder the corrosion of artificially patinated bronze [34], though their performances are significantly lower than that of BTA.

Continuing our work in this field and taking into account that the adsorptive behaviour of thiadiazole derivatives depends not only on their chemical/electronic structure, but also on the solution pH [36], in the present paper, we have examined the anticorrosive properties of the thiadiazole derivatives on naked and patina-covered bronze in an acidic carbonate/sulphate solution of pH 3, simulating the acidification reached on the metallic surface at the beginning of the rainfalls in much polluted urban environment [13]. For comparison reasons, the inhibiting effect of BTA was also examined. To the best of our knowledge,

no work has been documented on the impact of pH value in corrosive media on the interaction between thiadiazole molecules and bronze surface.

Electrochemical impedance spectroscopy (EIS) and SEM-EDX observations were used to evaluate the inhibiting efficiencies of thiadiazole derivatives and a quantum chemical calculation method was applied in an attempt to explain the influence of solution pH on the adsorption behaviour of the inhibitors and to correlate their structural and electronic characteristics with their experimental inhibition efficiencies.

2 Experimental methods

A three-electrode cell was used for the electrochemical experiments. The working electrode was made of a bronze cylinder rod ($S = 0.28 \text{ cm}^2$) with the following chemical composition (in wt%): Cu-93.66, Sn-6.10, Zn-0.10, Fe-0.02, Pb-0.01, P-0.11. The counter-electrode was a large platinum grid and a saturated calomel electrode (SCE) was used as reference electrode.

In order to avoid the electrolyte infiltration, the lateral part of the bronze rod was firstly protected by a cathaphoretic paint layer, cured at 150°C for 30 min. Then, the rod was embedded into an epoxy resin (Buhler, Epoxyure™). Prior to measurements, the working electrode was mechanically grounded using successive grade of silicon carbide paper up to grade 2400 to obtain a smooth and planar surface and then rinsed thoroughly with distilled water and ethanol.

The artificial patina was electrochemically synthesized on the bronze electrodes in an aerated solution of 0.2 g/L NaHCO_3 + 0.2 g/L Na_2SO_4 at 30°C , according to a procedure previously described [34]. The pH of the solution, as prepared was 8.5. This solution is expected to produce a patina characteristic for the urban environment. The SO_4^{2-} ions are one of the main pollutants in urban atmosphere due to the industrial activity and the car exhaust emission [33]. The EDX analyses of the patina showed that it may contain $\text{Cu}(\text{OH})$, SnO_2 or $\text{Sn}(\text{OH})_4$, sulphate and carbonate ions [34]. The green patina structure is well representative of the Type I corrosion structure found on ancient bronzes [3].

The electrochemical measurements were carried out in an aerated solution of 0.2 g/L Na_2SO_4 + 0.2 g/L NaHCO_3 , acidified to pH = 3 by addition of dilute H_2SO_4 . This corrosion test solution simulates an acidic rain, which could be found at the beginning of a rainfall in a polluted urban environment. Although one may consider that the solution pH is markedly acidic, it allows the occurrence of the corrosion process with a suitable rate [37].

The investigated thiadiazole derivatives compounds were: MAT, MMeT, MAcAT and MPhAT. The molecular structures of the thiadiazole derivatives were previously reported [35].

All solutions containing thiadiazole derivatives were prepared using distilled water and ethanol (90:10 v/v) from which appropriate volumes were introduced into the corrosive medium in order to obtain concentrations of 0.1; 1; 5 or 10 mM, depending on the organic compounds solubility limit. For comparison reasons, the inhibiting effect of BTA was also examined.

EIS measurements were conducted at the open circuit potential (E_{ocp}) after 1 h immersion of the electrode (naked bronze or artificially patinated specimens) in the corrosive solution, using

a PAR model 2273 potentiostat controlled by a PC computer. The impedance spectra were acquired in the frequency range 100 kHz to 10 mHz at 5 points per hertz decade with an AC voltage amplitude of ± 10 mV. ZSimpWin V3.21 software was used for fitting the experimental data using different equivalent electrical circuits.

Because slight variations in the patina composition of each patina-covered bronze sample might occur even if all electrodes were subjected to identical patina formation procedures, in order to compare uninhibited and inhibited samples, the experimental procedure previously described by Marusic et al. [32] was applied. Thus, the patinated bronze electrodes were first immersed in the corrosion test solution without inhibitor and after 1 h stabilization period, impedance spectra labelled 'blank' were collected. Then, the electrodes were dipped out from this solution, dried in air and dipped again in the corrosion solution containing organic inhibitors. The EIS spectra corresponding to inhibitor-containing solutions were time-monitored by EIS.

For morphological studies, the bronze surface was prepared by keeping the electrodes for 66 h in electrolytes containing the

optimum concentrations of inhibitors. Then, the specimens were gently washed with water, carefully dried and analysed without any further treatment, by scanning electron microscopy using a Zeiss Ultra 55 SEM FEG apparatus coupled with an EDS elemental semi-quantitative analyser.

The thiadiazole derivatives structures were investigated with the density functional theory (DFT) using hybrid B3LYP, 6-31G* model [38–40]. The following quantum chemical indices were considered: the energy of the highest occupied molecular orbital (E_{HOMO}), the energy of the lowest unoccupied molecular orbital (E_{LUMO}), energy band gap ($\Delta E = E_{\text{LUMO}} - E_{\text{HOMO}}$). The chemical quantum calculations were made using Spartan software [41].

3 Results and discussion

3.1 Naked bronze

3.1.1 Morphological analysis

In order to verify if the investigated thiadiazole derivatives act as inhibitors on the corrosion of naked bronze, both SEM and EDX

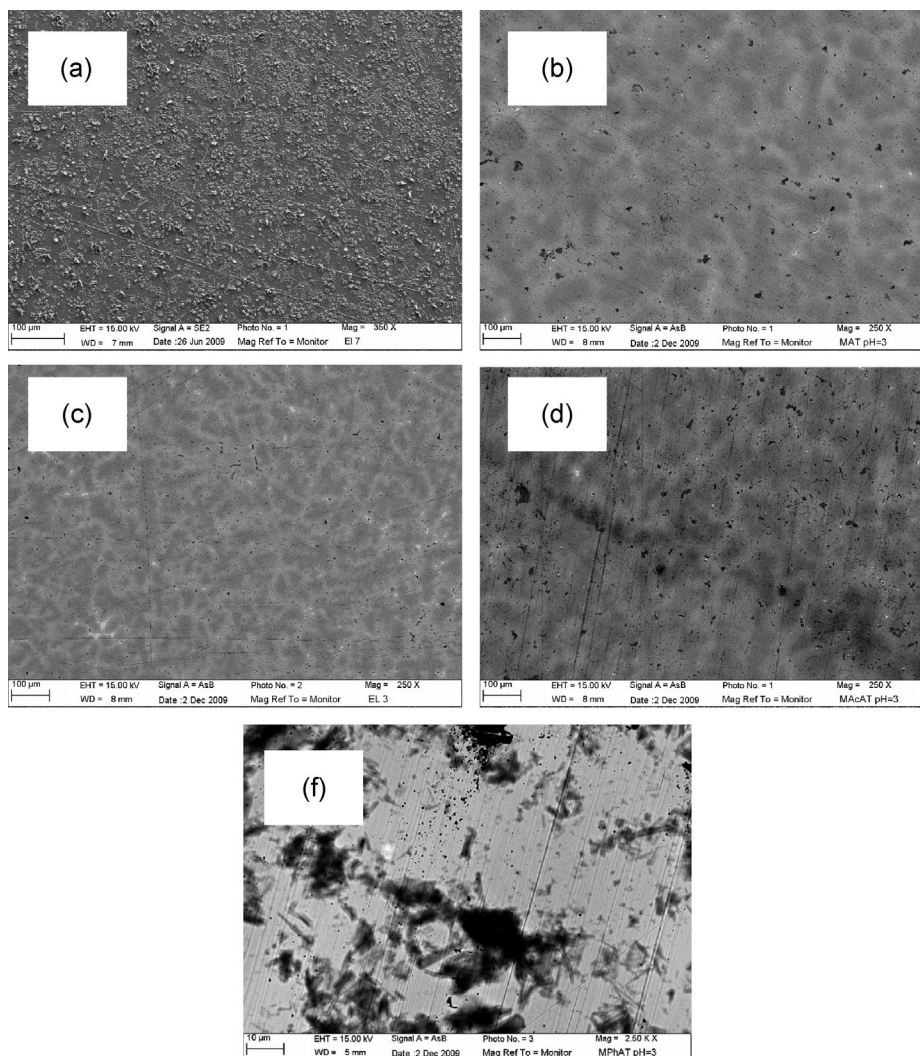


Figure 1. SEM micrograph of the naked bronze surface obtained after 66 h immersion in acidic carbonate/sulphate solution (pH 3) in the absence (a) and in the presence of (b) 5 mM MAT; (c) 5 mM MMeT; (d) 5 mM MACAT and (e) 1 mM MPhAT

experiments were carried out. Figure 1a presents the naked bronze surface morphology after 66 h of immersion in the corrosive solution in the absence of any organic compound. It can be seen that the bronze surface is covered with a layer of corrosion products. On contrary, in the presence of thiadiazole derivatives (Fig. 1b–e), no corrosion is observed on the bronze and the grooves due to the initial surface abrasion remain visible after 66 h immersion in the corrosive solution. The precipitates observed on the bronze surface immersed in the solution containing MPhAT are due to the insufficient electrode rising to avoid a wash-out of the corrosion products if they are present at the surface.

The bronze surface analysis by EDX (results not shown) reveals the presence of oxygen and sulphur in addition to the major elements (Cu, Sn and Zn) when the electrode was immersed in the reference solution (pH 3) during 66 h. The corrosion products would be mainly in the oxide form [42]. If the

bronze was dipped in the corrosive media containing thiadiazole derivatives, the peak due to oxygen significantly decreases, which proves that there are less corrosion products on the electrode surface. However, the EDX analysis of the bronze after its immersion in the corrosive solution in the presence of thiadiazole derivatives does not allow the identification of the organic compounds on the electroic surface.

3.1.2 Electrochemical impedance spectroscopy measurements

The protective effectiveness of the investigated thiadiazole derivatives on the bronze corrosion was evaluated by impedance spectroscopy measurements. The experiments were performed after 1 h of immersion in the corrosive solution (pH 3) to ensure the stability of the system during the impedance measurement [43].

Figure 2 presents the impedance spectra for naked bronze immersed in acidic carbonate/sulphate solution (pH 3) in the

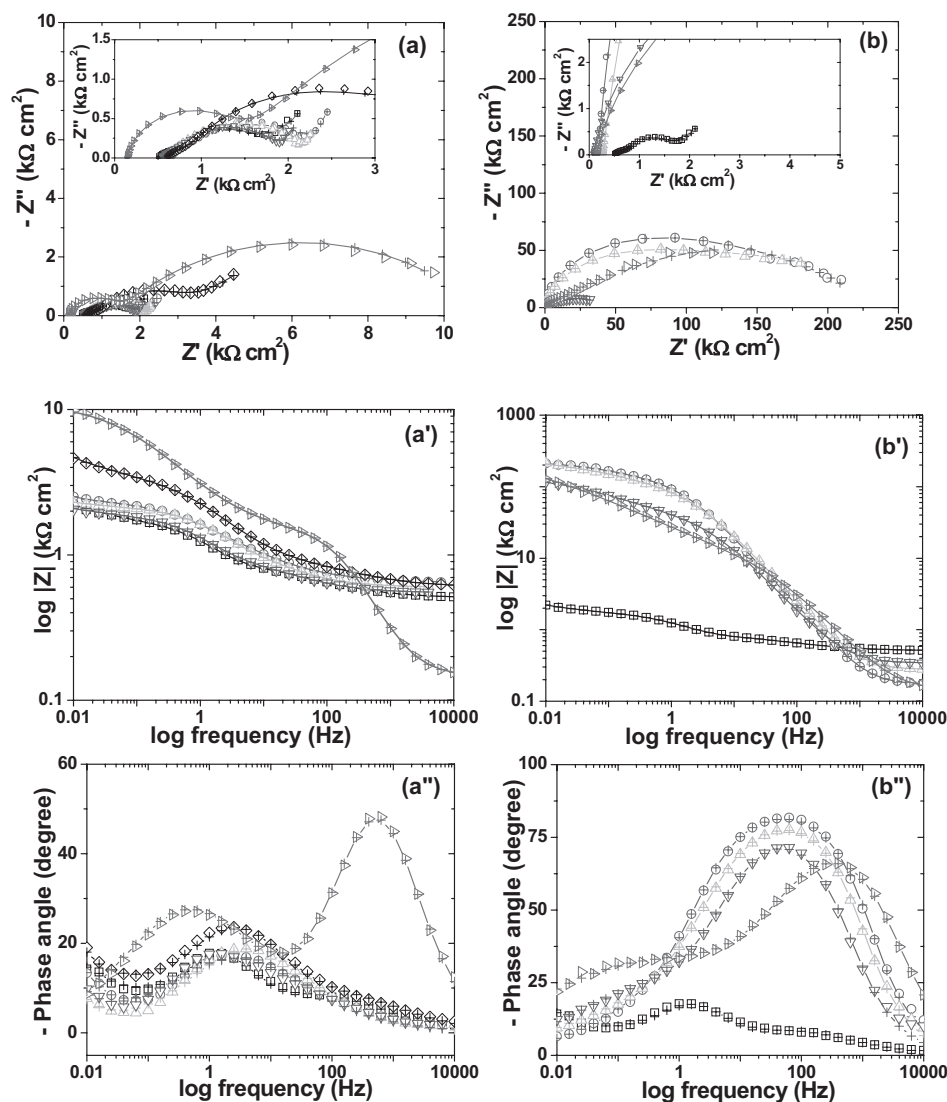


Figure 2. Nyquist and Bode plots for the corrosion of naked bronze in acidic carbonate/sulphate solution (pH 3) in the absence (□) and in the presence of organic inhibitors (mM): (○) MMeT; (△) MAT; (▽) MACAT; (◇) MPhAT; (▷) BTA, at various concentrations (mM): 0.1 (a–a'–a'') and 5 (b–b'–b''). Symbols corresponds to the experimental data and the line with cross (—+—) to the calculated data

absence and in the presence of organic inhibitors at the lowest (0.1 mM) and highest (5 mM) investigated concentrations, represented as Nyquist and Bode plots.

As it can be easily noticed in Fig. 2, the visual appearance of the Nyquist plots obtained for bronze corrosion in acidic solution (pH 3) depends on the organic inhibitors concentration. Thus, in the blank solution (pH 3) and in the presence of the lowest concentrations of thiadiazole derivatives, the impedance diagrams are characterized by a semicircular appearance with two badly separately capacitive loops, followed by a straight tail in the lowest frequency range. The inclination of the Warburg tail at around 45° to the real-axis in the low frequency region, suggests that in the pH 3 solutions, a diffusion process might occur at the bronze surface, probably due to the dissolved oxygen, and consequently the corrosion process is mixed controlled by charge transfer and diffusion.

At higher concentrations of thiadiazole derivatives (≥ 1 mM), a significant change of the impedance diagrams in both shape and size could be observed in Fig. 2. Thus, the diffusion impedance disappears by increasing the inhibitors concentration and a capacitive behaviour with depressed loops is evident in the whole frequency range. Disregarding the nature of the thiadiazole derivatives, a large increase of the impedance is evident at high concentrations of organic compounds compared to blank solution, pointing out to a strong inhibition of the bronze corrosion process, probably due to the adsorption of inhibitors on the metallic surface. The adsorbed layer of inhibitor could act as blocking barrier for bronze dissolution, possibly hindering the dissolved oxygen diffusion towards the bronze surface, as well. The disappearance of the Warburg impedance at high concentrations of organic compounds in the corrosive solution suggests a modification of the bronze dissolution mechanism, which might become controlled by the charge-transfer process, due to formation of a protective layer of inhibitor on the bronze surface [44].

The impedance data corresponding to the naked bronze corrosion in pH 3 electrolyte without and with the addition of the lowest concentration of thiadiazole derivatives were analysed in terms of the electrical equivalent circuit presented in Fig. 3a. In this model, R_e corresponds to the electrolyte resistance, the

parameter R_{ct} coupled with Q_d describe the charge transfer process at the electrolyte/bronze interface. The parameters R_F – Q_F are related to an oxidation–reduction process involving a reaction intermediate (i.e. Cu^+ ions) [25,32], while W stands for the Warburg impedance.

In order to model the bronze corrosion process in the presence of high concentrations of thiadiazole derivatives (≥ 1 mM) and in the presence of BTA, in a first attempt, it was assumed that the experimental data could be described by the same (3RC) electrical equivalent circuit that has previously been used to reproduce the impedance spectra obtained in the same carbonate/sulphate solution electrolytes at pH = 5 [35]. The results of the fitting procedures were found to be inappropriate in strong acidic solution (pH = 3). As formerly explained [35], in weakly acidic solution (pH 5) the high frequency loop (R_F – C_f) in the (3RC) circuit, was allocated to a surface oxide film layer (presumably Cu_2O and SnO_2) covering the bronze surface. In the pH 3 corrosive medium, the formation of a stable surface oxide layer on bronze is less probable due to the aggressiveness of the solution. According to Vastag et al. [45], copper can only be passivated in weakly acidic or alkaline solutions by forming an oxide surface layer. Hence, the impedance spectra corresponding to bronze corrosion in the presence of high concentrations of organic compounds were accurately fitted to a (2RQ) electrical equivalent circuit presented in Fig. 3b. The origins of the two R–Q couples were ascribed to the contributions mentioned above. A (2RC) ladder circuit was formerly used by Marusic et al. [32] to explain bronze corrosion in the presence of 4-methyl-1-*p*-tolylimidazole.

In the equivalent circuits from Fig. 3, instead of capacitance elements, we have used constant phase elements (CPEs) represented by the terms, Q and n . The use of CPEs as substitutes for pure capacitive elements is widely applied nowadays to account for the deviations induced by the surface roughness and various other non-homogeneities of the metallic surface [46], resulting from the presence of the impurities, inhibitor adsorption, formation of porous layer, insufficient polishing, etc.

The impedance of the CPEs is described by the following equation [47]:

$$Z_{\text{CPE}}(\omega) = [C(j\omega)n]^{-1} \quad (1)$$

where Q is a pre-exponential factor, which is a frequency-independent parameter with dimensions of $\Omega^{-1}/\text{cm}^2 \text{s}^n$; j is an imaginary number; $\omega = 2\pi f$ is angular frequency in rad/s; n is the exponent which defines the character of frequency-dependence ($-1 \leq n \leq 1$). The values of n are associated with the non-uniform distribution of current as a result of roughness and surface non-homogeneities.

The quality of fitting procedure was evaluated by the chi-squared (χ^2) values, which were of the order of 10^{-4} – 10^{-3} . Moreover, the error percentages corresponding to the component of the equivalent circuits were generally below 10%, indicating that the data adjusted well to the proposed equivalent circuit. Finally, a further confirmation of the fact that the used equivalent circuits correctly reproduce the experimental impedance corresponding to the bronze corrosion in strong acidic solution

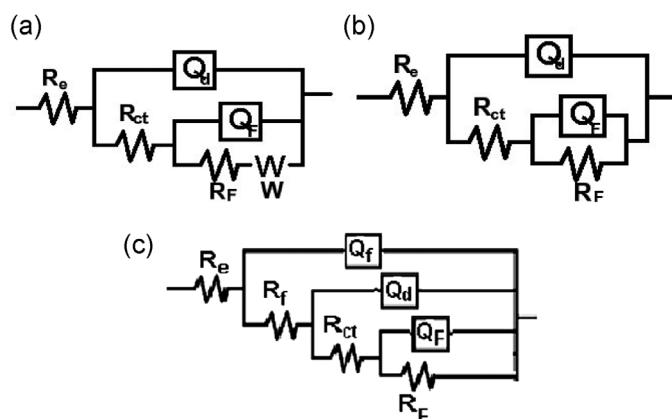


Figure 3. Equivalent electrical circuits used to reproduce the experimental data

without and with the addition of various concentrations of thiadiazole derivatives is revealed in Fig. 2, where a good agreement between the experimental and simulated data was obtained.

The values of the pseudo-capacitances associated with the CPEs were recalculated using the equation:

$$C = (R^{1-n}Q)^{1/n} \quad (2)$$

The variations of the calculated R and C parameters as a function of the thiadiazole derivatives concentration are illustrated graphically in Fig. 4. For comparison reasons, the fitting parameters obtained when BTA was used as bronze corrosion inhibitor in acidic solution (pH 3) were also included in Fig. 4.

In the blank solution (pH 3), the calculated value of capacitance C_d is $67.7 \mu\text{F}/\text{cm}^2$, plausible for a double layer capacitance, thus validating the model used for experimental data

simulation. Except for the case of 0.1 mM MPhAT, the addition of the lowest concentration of thiadiazole derivatives in the corrosive solution leads to a slight decrease of the double layer capacitance. The value of R_{ct} is $0.38 \text{ k}\Omega \text{ cm}^2$ in absence of the thiadiazole derivatives and remains almost unchanged at the thiadiazole derivatives concentration of 0.1 mM (Fig. 4a). By increasing the thiadiazole derivatives concentration, the C_d values progressively decrease as it can be seen in Fig. 4b. These results suggest that the inhibitors molecules act by adsorption mechanism at the bronze/acid interface. The surface coverage by organic compounds may deeply change the double layer structure [48], thus explaining the considerable lowering of the C_d values at high concentrations of thiadiazole derivatives. On the other hand, the R_{ct} values increase steeply and acquire their greatest values in the solutions containing the optimum level of thiadiazole derivatives, i.e. 5 mM for MAcAT, MAT or MMeT and 1 mM for MPhAT. The significant increase of the R_{ct} values by

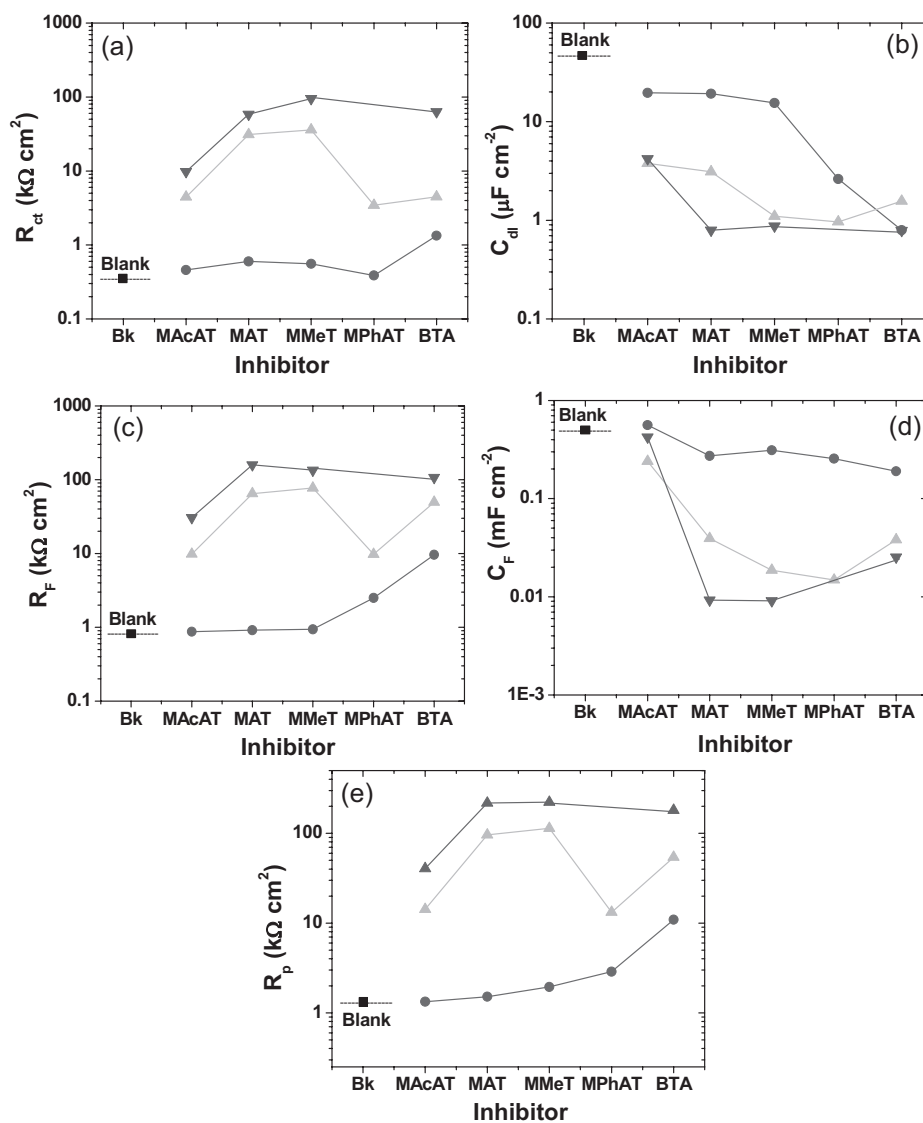


Figure 4. Evolution of the R - C parameters calculated for naked bronze in acidic carbonate/sulphate solution (pH 3), as a function of the organic inhibitors concentration (mM): (■) 0; (●) 0.1; (▲) 1; (▼) 5

addition of higher concentrations of thiadiazole derivatives could be related to the strong anticorrosive properties of these compounds in acidic electrolytes. The best protective effect was observed in the presence of MMeT. The R_{ct} value was almost 250 times higher when 5 mM MMeT was added into the corrosive solution compared to its absence. Nevertheless, a decrease of the R_{ct} value from 94.9 to 64.1 k Ω cm² was put on evidence by increasing the MMeT concentration from 5 to 10 mM (results not shown). A similar behaviour was observed for other inhibitors [49,50] and it might be caused by the deterioration of the adsorbed film on the bronze surface [51].

In the presence of the organic compounds at their lowest concentrations, the values of R_F and C_F are only slightly higher compared to those calculated in inhibitor-free solution, which means that the studied compounds exert a small protective effect towards the redox process preceding the dissolution step of the reaction intermediate. With increasing the inhibitors concentration, the R_F values increase sharply, while simultaneously the C_F values continuously decrease (Fig. 4c and d). The faradaic resistances attain their maximum values in solutions containing the highest concentrations of thiadiazole derivatives. In the same time, at these concentrations, the faradaic capacitances reach the minimum values, which could be a consequence of the fact that not the whole surface species are involved in the redox process taking place at the electrodic surface, due to the inhibitive adsorption of the organic compounds [48]. Thus, the adsorbed molecules could impede to some extent the formation of corrosion products and in parallel may stabilize the species covering the electrode, which became less susceptible to the redox processes and provide enhanced protection to the bronze surface. This explains the absence of the corrosion products on the SEM micrographs obtained in the presence of the thiadiazole derivatives (Fig. 1) and why it was practically impossible to qualitatively identify the nitrogen atoms in the EDX spectra of the bronze exposed to inhibitor-containing solutions.

The variation of the polarisation resistance values, R_p , calculated as the sum of the resistances, R_{ct} and R_F is shown in Fig. 4e as a function of the organic inhibitors concentration.

The R_p values were used to calculate the inhibition efficiency, z , as a function of the thiadiazole derivatives concentration (Table 2), according to following equation:

$$z = \frac{R_p^0 - R_p}{R_p^0} \quad (3)$$

where R_p and R_p^0 are the polarization resistances in electrolytes with and without inhibitors, respectively.

As it is shown in Fig. 4e, the inhibitive effect of the investigated thiadiazole derivatives is scarce at their lowest concentrations (0.1 mM). This can be explained as there is a partial diffusion control of the dissolution process, which means that at low concentrations of organic compounds the inhibition degree might be limited not only by the partial coverage of the electrode surface with adsorbed thiadiazole derivatives, but also by the oxygen diffusion process [52]. The substantial increase of the inhibition efficiency values observed at high concentrations of inhibitors (≥ 1 mM) could be due to the formation of a highly protective layer of the organic compounds on the bronze surface that prevents the diffusion process and significantly decreases the bronze corrosion rate.

In the investigated experimental conditions, at their optimal concentrations (5 mM), MMeT and MAT show a more protective effectiveness on bronze corrosion compared to BTA.

Nevertheless, it should be noticed that the inhibition efficiency order of the investigated thiadiazole derivatives in 0.2 g/L Na₂SO₄ + 0.2 g/L NaHCO₃ acidified to pH = 3 is different compared to that obtained in weakly acidic electrolytes (pH 5) containing the same concentrations of inhibitors (Table 1) [35].

It can be observed that, in acidic solution (pH 3) MPhAT at concentration of 1 mM shows the lowest inhibitive efficiency among the tested compounds, while in weakly acidic solution (pH 5) it was proved to be the best inhibitor at 0.1 mM concentration range. Additionally, in most cases, the inhibition efficiencies obtained at concentrations of inhibitors ≥ 1 mM have greater values in pH 3 solution as compared to those calculated in pH 5 electrolyte.

There is no doubt from these results that the action mechanism of the investigated thiadiazole derivatives is strongly dependent on the corrosive solution pH, as well as on their molecular structure, particularly on the electronic structure. Consequently, in the next part of the work, quantum chemical calculations will be used in order to explain the differences in the experimental behaviour of the thiadiazole derivatives on bronze corrosion process at different pH values of the corrosive solution.

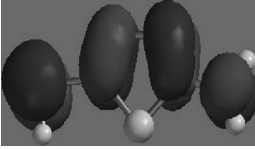
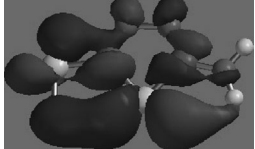
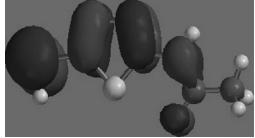
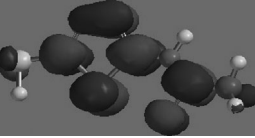
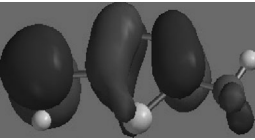
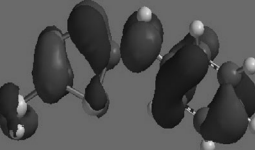
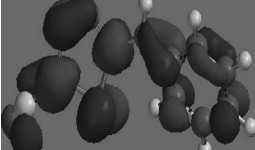
3.1.3 Quantum chemical calculations

In order to find a possible correlation between the experimental inhibition efficiencies and the electronic structures of the thiadiazole inhibitors, the minimum energy geometry of each

Table 1. Influence of the corrosive solution pH and of the organic inhibitors concentration on the inhibition efficiency values

Inhibitor conc. (mM)	z (%)								
	MMeT		MAT		MAcAT		MPhAT		BTA
	pH								
	3	5	3	5	3	5	3	5	3
0.1	38.9	86.5	21.6	-13.8	10.8	-7.8	58.8	97.0	89.1
1	98.95	91.1	98.76	88.5	91.7	95.7	90.9	42.2	96.9
5	99.48	92.6	99.36	95.9	97.0	-	-	-	99.06

Table 2. Theoretical quantum chemical parameters of the thiadiazole derivatives and typical HOMO and LUMO densities distribution

Molecule	E (au)	E_{HOMO} (eV)	HOMO densities distribution	E_{LUMO} (eV)	LUMO densities distribution	ΔE (eV)
MAT	-1038.60565	-5.89		-0.88		5.01
MAcAT	-1191.27241	-6.31		-1.17		5.14
MMeT	-1022.57308	-6.70		-1.11		5.59
MPhAT	-1269.65850	-5.88		-1.20		4.68

derivative has been obtained starting with molecular mechanics optimization of the conformers generated within the Confanal module of Spartan'06 [41], followed by semi-empirical (PM3), HartreFock and 6-31G(d) B3LYP DFT [38–40]. The generated lowest energy conformers were further used in order to calculate the quantum molecular parameters, such as E_{HOMO} , E_{LUMO} and the ΔE energy gap, which are given in Table 2.

The theoretical data obtained by B3LYP, 6-31G(d) level of theory (Table 2), show that the values of the energy band gap (ΔE) for the thiadiazole derivatives in the pH 5 solution lay in the following order: MPhAT > MAT > MAcAT > MMeT and are in good agreement with the calculated values of the inhibition efficiencies.

Modifications of the corrosion inhibition efficiencies of thiadiazole derivatives at pH 3 are most probably due to structural changes in the thiadiazole moiety following the protonation at one of the nitrogen atoms in the heterocycle. The protonation equilibria of the thiadiazole derivatives which may occur in acidic media (pH 3) are presented in Scheme 1.

The protonated structures of the thiadiazole derivatives and BTA in acidic media (pH 3) were simulated based on DFT using hybrid B3LYP, 6-31G(d) and the calculated quantum parameters, such as E_{HOMO} , E_{LUMO} , ΔE are given in Table 3. Moreover, in an attempt to determine the most stable protonated thiadiazole moiety, the total energy E of the isomers were calculated and the species characterized by the lowest energy values were selected and included in Table 3.

According to E values in Table 3 the protonation of the N2-nitrogen atom in the thiadiazole ring appears to be favoured in all cases, exception for MAT-derivative, probably due to the electron

donor effect of the amino ($-\text{NH}_2$) substituent in position 5 of the heterocycle which orients the protonation towards N1. In the case of BTA, the protonation takes place at N3 atom and the calculated value of ΔE is -4.775 eV.

The theoretical results obtained by B3LYP, 6-31G(d) method (Table 3) show that ΔE for the protonated species of thiadiazole derivatives and BTAH⁺ lay in the following order: MMeT

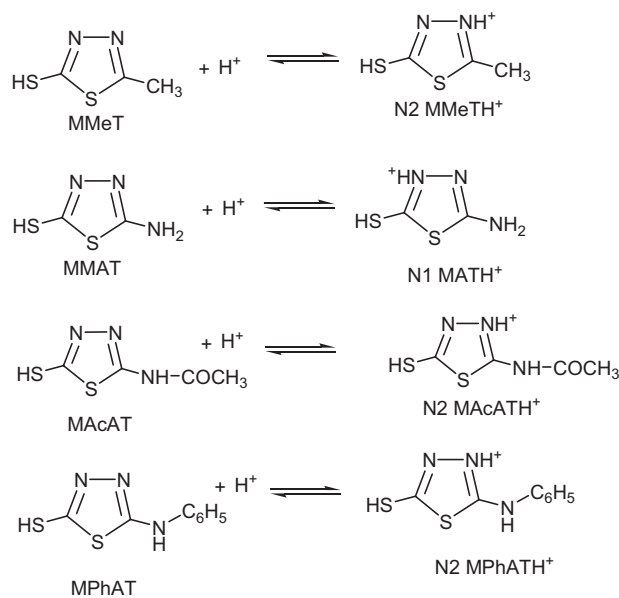
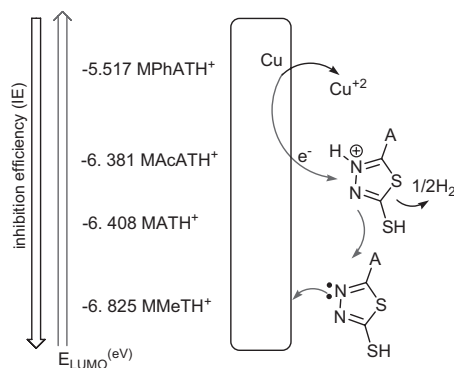
**Scheme 1.** Protonation equilibrium of the thiadiazole derivatives in acidic media (pH 3)

Table 3. Theoretical quantum chemical parameters of the protonated thiaziazole derivatives and typical HOMO and LUMO densities distribution

Compound	Protonated position	E (au)	E_{HOMO} (eV)	HOMO densities distribution	E_{LUMO} (eV)	LUMO densities distribution	ΔE (eV)
MMeT H ⁺	N2	-1022.9319	-11.528		-6.825		4.703
MAT H ⁺	N1	-1038.9718	-11.173		-6.408		4.765
MAcAT H ⁺	N2	-1191.6196	-11.197		-6.381		4.816
MPhAT H ⁺	N2	-1270.0338	-10.561		-5.517		5.044

$\text{H}^+ > \text{MATH}^+ > \text{BTAH}^+ > \text{MAcAT H}^+ > \text{MPhAT H}^+$ pointing in the same direction as the inhibition efficiency values obtained from EIS technique (Table 1).

A possible mechanism of inhibition performed by the thiaziazole protonated species existing at pH 3 is suggested in Scheme 2 and involves in the first step a cathodic reduction on the bronze surface generating the neutral thiaziazole ring which further coordinates the copper on the surface. The facility of the reduction processes may be directly correlated with the LUMO orbital energy, a lower energy value suggesting the easiness in accommodating the incoming electrons. The crucial electrochemical reduction step is followed by fast free thiaziazole base formation. According to the proposed mechanism, the experimental increase in inhibition efficiencies should be correlated with the decreasing LUMO energy, a fact which was supported by both experimental and theoretical data (Tables 1 and 3).

**Scheme 2.** The possible mechanism of inhibition performed by the thiaziazole protonated species

Another aspect that should be taken into consideration at pH 3 is the increasing of the water solubility of the thiaziazole derivative after the protonation to the nitrogen atom in thiaziazole ring. Additionally, it can be seen that the value of the energy band gap ΔE , for the protonated thiaziazoles at pH = 3 is generally lower than that corresponding to pH = 5. Consequently, the inhibition mechanism at pH 3 is different from that noticed at pH 5.

3.2 Bronze covered by artificial patina

The promising results obtained in the first part of the paper revealing that MMeT and MAT exert a higher inhibiting efficiency on bronze corrosion in acidic carbonate/sulphate corrosive solution (pH 3) than the harmful but widely-used BTA determined us to investigate the effect of these organic compounds on bronze covered with artificial patina. For this purpose, electrochemical impedance spectra corresponding to the artificially patinated bronze electrodes were recorded every 2 h during the first 24 h and then every day up to 14 or 28 days of immersion in acidic corrosive solution (pH 3), without and with the addition of MMeT, MAT and BTA. Prior to the impedance measurements, the samples were left at the open-circuit potential for 1 hour in the corrosive solution.

Figure 5 illustrates typical impedance spectra of the bronze covered with artificial patina, obtained after different exposure times in the corrosive electrolyte (pH 3), in the absence and in the presence of the tested organic compounds at a concentration of 5 mM. The results are displayed as Nyquist and Bode plots.

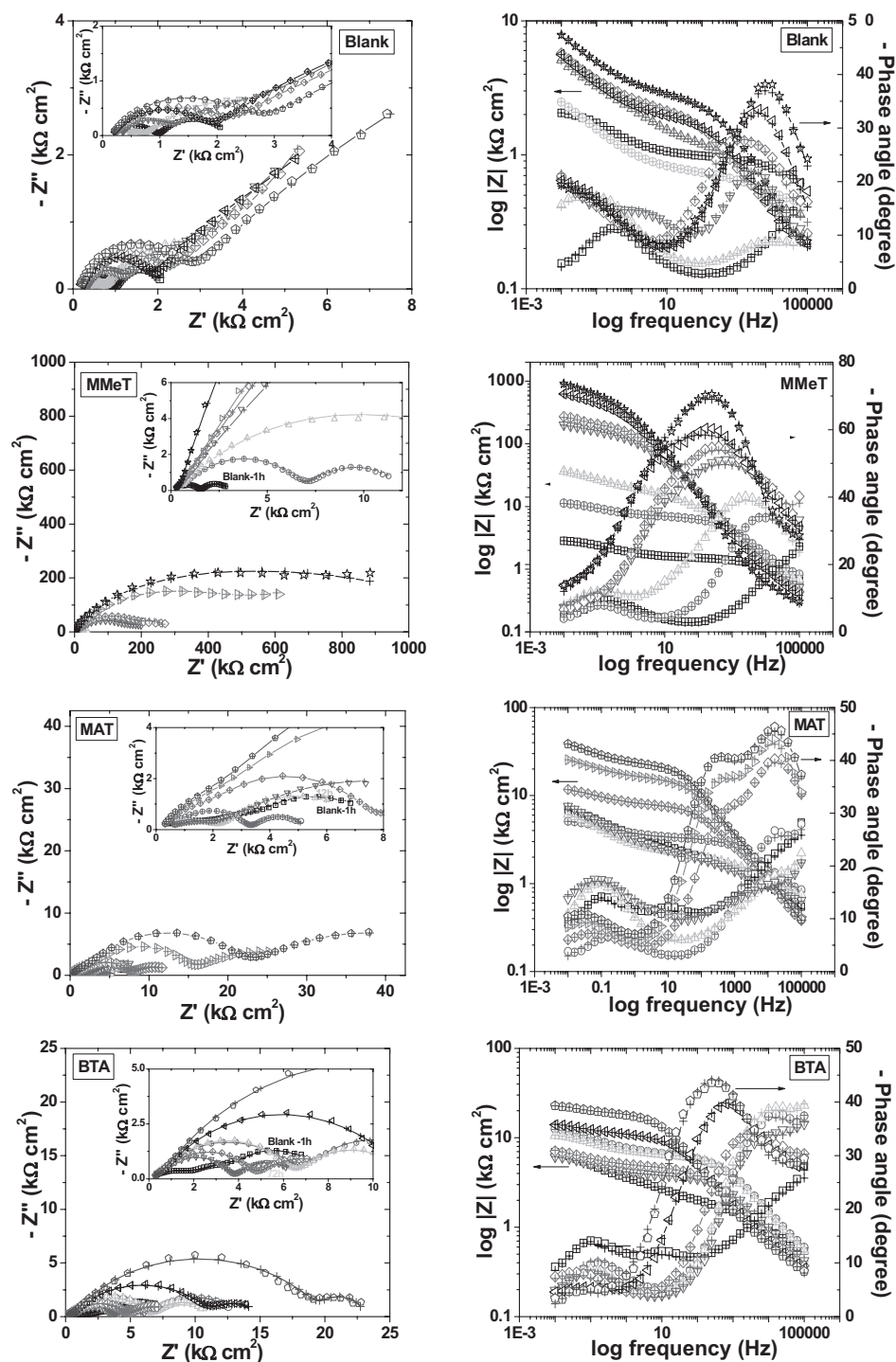


Figure 5. Nyquist and Bode plots for the corrosion of the bronze covered with artificial patina in acidic carbonate/sulphate solution (pH 3) in the absence ('blank-1 h') (\square) and in the presence of the organic inhibitors (5 mM), obtained at different exposure times (h): (\odot) 1; (\triangle) 12; (∇) 24; (\diamond) 72; (\triangleright) 120; (\triangleleft) 168; (\triangle) 336; (\star) 672. Symbols corresponds to the experimental data and the line with cross ($-+ -$) to calculated data

All impedance spectra exhibit a capacitive behaviour with depressed semicircles over the whole frequency range. The significant increases of the impedance modulus $|Z|$ of the artificially patinated bronze samples exposed to inhibitor-containing solutions compared to the $|Z|$ value obtained in the reference solution confirm the protective effect of the tested

compounds. In addition, a marked change of the impedance diagrams in size and shape with time could be noticed both in the absence and in the presence of the inhibitors. Thus, during the early stages of immersion in acidic carbonate/sulphate solution (pH 3), the impedance response of the patinated bronze specimens is characterized by a capacitive behaviour with two

well-separated loops, but on continued immersion the appearance of a diffusion tail becomes evident at low frequencies (Fig. 5a). Consequently, depending on the length of the exposure time, the EIS data recorded in the absence of any inhibitor for the bronze electrode covered with artificial patina were interpreted according to the two equivalent circuits depicted in Fig. 3a and b. The equivalent circuit from Fig. 3b was used to fit the EIS data displaying two capacitive loops, while the one from Fig. 3a was used for the EIS data displaying diffusion impedance.

In the presence of the organic inhibitors, three capacitive loops, though badly separated from each other could be observed at all exposure times. Accordingly, these data were tentatively represented by the electrical equivalent circuit also depicted in Fig. 3c and named (3RQ) circuit. Compared to the (2RQ) circuit used for fitting the EIS data of naked bronze exposed to inhibitor-containing solution, the (3RQ) circuit proposed for patinated specimens includes an additional R_f - Q_f couple, which appears in the highest frequency domain and was ascribed to an insulating layer with certain ionic conduction [32,33]. The parameter Q_f represents the CPE related to the film capacitance due to its dielectric nature, while the resistance of the surface film, R_f indicates the ionic leakage through the oxide/adsorbed inhibitor layer. The origin of the other parameters from the (3RQ) equivalent circuit was ascribed to the same contributions as in the case of the (2RQ) circuit.

As it can be seen in Fig. 5, the calculated EIS data overlap well with the experimental ones, at different exposure times, validating the models used in the fitting procedure. However, in some cases, the high frequency limit of the impedance measured at low exposure time did not allow a reliable determination of the solution resistance value and, therefore, the corresponding R_c values were kept at fixed values. It should be also mentioned that in some cases, at low immersion times, it was difficult to unambiguously calculate the parameters R_f and C_f corresponding to the first time constant from the impedance diagrams obtained in inhibitor-containing solution. For improving the fitting procedure, the n_1 values were fixed at 0.8.

The protective properties of the investigated thiadiazole derivatives were estimated by studying the variation of the charge transfer resistance, R_{ct} and polarisation resistance, R_p with

respect to the exposure time of the bronze covered with artificial patina in acidic corrosive solution (pH 3), as shown in Fig. 6.

As explained in previous papers [31,53], in the presence of the oxidation-reduction process at the electrode surface, the polarization resistance R_p , determined as the sum of three resistances determined by the regression calculation is the parameter the most closely related to the corrosion rate, while the charge transfer resistance, R_{ct} indicates the current exchange taking place at the electrode surface covered with artificial patina.

All investigated organic compounds retard the corrosion of bronze covered with artificial patina and this effect is time-dependent, as revealed in Fig. 6, where an increase of the R_{ct} and R_p values is noticeable during the entire exposure period in inhibitors-containing solution, compared to the reference solution.

For unprotected patinated bronze, the R_{ct} values are low at the beginning of exposure (in the first 14 h) to the acidic corrosive solution (pH 3), then slightly increase up to 72 h of immersion and become almost constant after 6 days of exposure. In the case of the patinated specimen immersed in MMeT-containing solution, the R_{ct} values increase significantly with the immersion time up to 96 h and stabilize at a value nearly 334 times higher than that corresponding to the unprotected bronze. A similar variation was observed for the R_f values, which constantly increase with the immersion time (results not shown).

The inhibitive effect of MAT is relatively low in the first hours of immersion, but it continuously increases during time and became considerable after one week. The high values of R_{ct} obtained at long exposure times suggests that MAT slows down the electrochemical process taking place at the artificially patinated bronze surface, probably by stabilizing the oxide layers.

The protective effect of BTA on the patinated bronze is almost identical to that exerted by MMeT at the beginning of immersion in the acidic corrosive medium (pH 3), then slightly increases up to 6 h, as revealed by the increases of the R_{ct} values, but after that it starts to decrease with further increases of the exposure time to one day and finally stabilizes at longer immersion period. The results of our investigations are in agreement with some literature statements [54] reporting that in certain exposure conditions, BTA progressively loses its protection ability over time. A stabilization of the corrosion products covering the bronze surface in BTA-

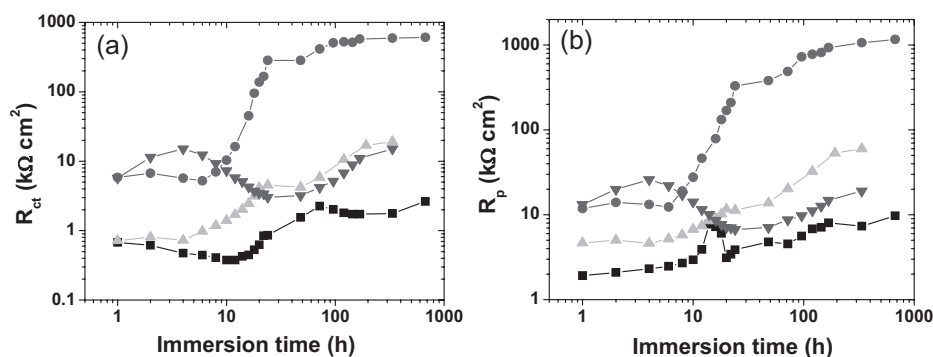


Figure 6. Time-changes of the charge transfer resistance (a) and of the polarization resistance (b) of the bronze samples covered with the artificial patina, in acidic carbonate/sulphate solution (pH 3) in the absence (■) and in the presence of the organic inhibitors (5 mM): MMeT (●); MAT (▲); BTA (▼)

containing solutions was observed at longer exposure times up to 336 h, probably due to the ageing effects, as a consequence of the dissolution of the most reactive species in the electrolyte and transformation of corrosion products into more stable compounds [48].

The variation of the polarization resistance values (Fig. 6b) shows that BTA protects slightly better the artificial patina covering the bronze electrode in the first 8 h of immersion in acidic carbonate/sulphate solution compared to MMeT and MAT. This ranking contrasts to those presented above with naked bronze and may possibly be a consequence of the fact that in some cases, especially at low immersion times, the R_p values are not always completely reliable. However, as the immersion time increases, the protective efficiency of the investigated organic inhibitors can be ranked as follows: MMeT > MAT > BTA.

Considering that BTA is a harmful substance that gradually loses its protection ability during long exposure time, the anticorrosive effect exerted by MMeT and MAT was considered adequate to preserve the bronze covered with patina.

4 Conclusions

Completing our previously reported results referring to thiadiazole derivatives as efficient inhibitors of bronze corrosion in weakly acidic solution (pH 5), the results obtained in the present paper showed that the anticorrosive performances of these inhibitors are affected by the pH of the corrosive solution, since these compounds appear to be protonated in stronger acidic medium. In an attempt to better understand the influence of solution pH on the adsorption of the thiadiazole derivatives and to correlate their structural and electronic characteristics with the experimental inhibition efficiencies, the thiadiazole derivatives structures were investigated by DFT using hybrid B3LYP, 6-31G* model. A possible inhibition mechanism of the thiadiazole protonated species on bronze corrosion was proposed.

In the investigated experimental conditions, MMeT was proved to be the most promising corrosion inhibitor to be applied both on naked and artificially patinated bronze. Moreover, MMeT and MAT allow the stabilization of the patina layer leading to the protection of the bronze substrate and their effectiveness significantly increases with the immersion time in acidic corrosive solution (pH 3). Contrarily, BTA progressively loses its protection ability over time.

Acknowledgements: The financial support within the project PN II IDEI code 17/2009 is gratefully acknowledged. The authors thank *Stephan Borensztajn* (CNRS – UPR 15) for his efficient help for SEM and EDX observation.

5 References

- [1] E. Bernardi, C. Chiavari, B. Lenza, C. Martini, L. Morselli, F. Ospitali, L. Robbiola, *Corros. Sci.* **2009**, *51*, 159.
- [2] C. Chiavari, K. Rahmouni, H. Takenouti, S. Joiret, P. Vermaut, L. Robbiola, *Electrochim. Acta* **2007**, *52*, 7760.
- [3] L. Robbiola, J. M. Blengino, C. Fiaud, *Corros. Sci.* **1998**, *40*, 2083.
- [4] B. Rosales, R. Vera, G. Moriena, *Corros. Sci.* **1999**, *41*, 625.
- [5] A. Vlasa, S. Varvara, L. Muresan, *Studia Univ. Babeş-Bolyai Chem.* **2007**, *LII*, 63.
- [6] A. Kratschmer, I. Odnevall-Wallinder, C. Leygraf, *Corros. Sci.* **2002**, *44*, 425.
- [7] M. Wadsak, T. Aastrup, I. Odnevall Wallinder, C. Leygraf, M. Schreiner, *Corros. Sci.* **2002**, *44*, 791.
- [8] G. Bierwagen, T. J. Shedlosky, K. Stane, *Prog. Org. Coat.* **2003**, *48*, 289.
- [9] M. Watanabe, E. Toyoda, T. Handa, T. Ichino, N. Kuwaki, Y. Higashi, T. Tanaka, *Corros. Sci.* **2007**, *49*, 766.
- [10] N. Souissi, L. Bousselmi, S. Khosrof, E. Triki, *Mater. Corros.* **2006**, *57*, 794.
- [11] H. Strandberg, *Atmos. Environ.* **1998**, *32*, 3511.
- [12] E. Sidot, N. Souissi, L. Bousselmi, E. Triki, L. Robbiola, *Corros. Sci.* **2006**, *48*, 2241.
- [13] L. Robbiola, K. Rahmouni, C. Chiavari, V. Martini, D. Prandstraller, A. Texier, H. Takenouti, P. Vermaut, *Appl. Phys.* **2008**, *A 92*, 161.
- [14] C. Chiavari, A. Colledan, A. Frignani, G. Brunoro, *Mater. Chem. Phys.* **2006**, *95*, 252.
- [15] T. Kosec, H. Otmacić Ćurković, A. Legat, *Electrochim. Acta* **2010**, *56*, 722.
- [16] M. C. Bernard, S. Joiret, *Electrochim. Acta* **2009**, *54*, 5199.
- [17] G. Bertolotti, D. Bersani, P. P. Lottici, M. Alesiani, T. Malcherek, J. Schlüter, *Anal. Bioanal. Chem.* **2012**, *402*, 1451.
- [18] E. Cano, D. Lafuente, D. M. Bastidas, *J. Solid State Electrochem.* **2010**, *14*, 381.
- [19] O. Olivares-Xometl, N. V. Likhanova, M. A. Domínguez Aguilar, E. Arce, H. Dorantes, P. Arellanes-Lozada, *Mater. Chem. Phys.* **2008**, *110*, 344.
- [20] R. B. Faltermeier, *SSCR J.* **1998**, *9*, 1.
- [21] R. B. Faltermeier, *Stud. Conserv.* **1998**, *44*, 121.
- [22] S. Varvara, M. Popa, G. Rustoiu, R. Axinte, L. M. Muresan, *Studia Univ. Babeş-Bolyai Chem.* **2009**, *54*, 73.
- [23] M. Finšgar, I. Milošev, *Corros. Sci.* **2010**, *52*, 2737.
- [24] I. Dugdale, J. B. Cotton, *Corros. Sci.* **1963**, *3*, 69.
- [25] G. Laguzzi, L. Luvidi, *Surf. Coat. Technol.* **2010**, *204*, 2442.
- [26] K. F. Khaled, *Corros. Sci.* **2010**, *52*, 3225.
- [27] S. Golfomitsou, J. F. Merkel, *presented at METAL'04*, Canberra, Australia, 4–8 October **2004**, pp. 344–368.
- [28] G. Brunoro, A. Frignani, A. Colledan, C. Chiavari, *Corros. Sci.* **2003**, *45*, 2219.
- [29] A. Balbo, C. Chiavari, C. Martini, C. Monticelli, *Corros. Sci.* **2012**, *59*, 204.
- [30] D. Zhang, L. Gao, G. Zhou, K. Y. Lee, *J. Appl. Electrochem.* **2008**, *38*, 71.
- [31] K. Rahmouni, H. Takenouti, N. Hajjaji, A. Srhiri, L. Robbiola, *Electrochim. Acta* **2009**, *54*, 5206.
- [32] K. Marusic, H. Otmacić-Curkovic, H. Takenouti, *Electrochim. Acta* **2011**, *56*, 7491.
- [33] K. Marusic, H. Otmacić-Curkovic, H. Takenouti, A. D. Mance, E. Stupnišek-Lisac, *Chem. Biochem. Eng.* **2007**, *21*, 71.
- [34] L. Muresan, S. Varvara, E. Stupnišek-Lisac, H. Otmacić, K. Marusic, S. Horvat-Kurbegovic, L. Robbiola, K. Rahmouni, H. Takenouti, *Electrochim. Acta* **2007**, *52*, 7770.
- [35] S. Varvara, L. M. Muresan, K. Rahmouni, H. Takenouti, *Corros. Sci.* **2008**, *50*, 2596.
- [36] H. Otmacić Curkovic, E. Stupnišek-Lisac, H. Takenouti, *Corros. Sci.* **2010**, *52*, 398.

- [37] K. Rahmouni, S. Joiret, L. Robbiola, A. Srhiri, H. Takenouti, V. Vivier, *presented at Advanced Techniques for Energy Sources Investigation and Testing*, Sofia, Bulgaria, 4–9 September 2004, pp. P8-1-11.
- [38] D. J. Becke, *Chem. Phys.* **1993**, *98*, 5648.
- [39] C. Lee, W. Yang, R. G. Parr, *Phys. Rev.* **1988**, *B37*, 785.
- [40] P. J. Stephens, F. J. Devlin, C. F. Chabulowski, M. J. Frisch, *Phys. Chem.* **1994**, *98*, 11623.
- [41] SPARTAN'06 Wavefunction, Inc., Irvine, CA **2006/2007**.
- [42] A. Dermaj, N. Hajjaji, S. Joiret, K. Rahmouni, A. Srhiri, H. Takenouti, V. Vivier, *Electrochim. Acta* **2007**, *52*, 4654.
- [43] H. Saifi, M. C. Bernard, S. Joiret, K. Rahmouni, H. Takenouti, B. Talhi, *Mater. Chem. Phys.* **2010**, *120*, 661.
- [44] M. A. Amin, K. F. Khaled, *Corros. Sci.* **2010**, *52*, 1194.
- [45] Gy. Vastag, E. Szocs, A. Shaban, I. Bertoti, K. Popov-Pergal, E. Kalman, *Solid State Ionics* **2001**, *87*, 141.
- [46] A. K. Singh, M. A. Quraishi, *Corros. Sci.* **2010**, *52*, 1373.
- [47] I. D. Raistrick, J. R. MacDonald, D. R. Franceschetti, *Impedance Spectroscopy Emphasizing Solid Materials and Systems*, Wiley, New York **1987**, pp. 27–84.
- [48] K. Marusic, *Ph. D. Thesis*, University of Zagreb, Croatia **2010**.
- [49] K. M. Ismail, *Electrochim. Acta* **2007**, *52*, 7811.
- [50] R. Bostan, S. Varvara, L. Gaina, L. M. Muresan, *Corros. Sci.* **2012**, *63*, 275.
- [51] D. Q. Zhang, Q. R. Cai, X. M. He, L. X. Gao, G. S. Kim, *Mater. Chem. Phys.* **2009**, *114*, 612.
- [52] K. F. Khaled, *Appl. Surf. Sci.* **2008**, *255*, 1811.
- [53] I. Epelboin, C. Gabrielli, M. Keddam, H. Takenouti, *Electrochemical Corrosion Testing*, American Society for Testing and Materials, Philadelphia STP 727 **1981**, pp. 150–192.
- [54] W. A. Mohamed, N. M. Rateb, A. A. Shakour, *presented at METAL'04, Canberra, Australia, 4–8 October 2004*, pp. 369–378.

(Received: February 15, 2013)

W7072

(Accepted: March 18, 2013)